Record, M. T., Jr., Anderson, C. F., & Lohman, T. M. (1978) *Q. Rev. Biophys. 11*, 103–178.
Record, M. T., Jr., Mazur, S. J., Melançon, P., Roe, J.-H., Shaner, S. L., & Unger, L. (1981) *Annu. Rev. Biochem. 50*, 997–1024.
Reuben, J., Shporer, M., & Gabbay, E. J. (1975) *Proc. Natl. Acad. Sci. U.S.A. 72*, 245–247.
Studier, F. W. (1969) *J. Mol. Biol. 41*, 199–209.
Wilson, R. W., Rau, D. C., & Bloomfield, V. A. (1980) *Biophys. J. 30*, 317–324.

Investigation of the Metastable Phase Behavior of Phosphatidylglycerol with Divalent Cations by Calorimetry and Manganese Ion Binding Measurements†

Joan M. Boggs* and Godha Rangaraj

ABSTRACT: Divalent cations induce a stable, dehydrated phase in phosphatidylglycerol only at a bound cation to lipid mole ratio equal to or greater than 0.5:1, suggesting that all of the lipid must be neutralized by the cation. However, after melting of the stable phase at high temperature, it refreezes into a metastable phase if cooled rapidly. The transition temperature of the metastable state, both on cooling and on reheating, is not quite as high as that of the lipid in its protonated state, indicating that the lipid is no longer completely neutralized. This suggested that a portion of the divalent cation dissociates from the liquid-crystalline phase and does not rebind to the gel phase of the metastable state. The transition from the metastable to the stable state is exothermic and occurs on heating. Its rate increases with increase in divalent cation concentration and is decreased by Na^+, suggesting that the dissociated divalent cation rebinds during the endothermic or exothermic transitions of the metastable phase, when the lateral motion of the lipid increases. Rebinding of the cation allows more complete neutralization of the lipid head groups, close approach of opposing bilayers, and formation of the stable dehydrated state. Measurement of Mn^{2+} binding at different temperatures from the electron paramagnetic resonance spectrum of Mn^{2+} confirmed this hypothesis. These results indicate that if the rate of lateral motion is low, the affinity of acidic lipids for divalent cations decreases as the available free lipid becomes diluted by cation-bound lipid or other membrane constituents.

Complexation of divalent cations with acidic lipids results in dehydrated bilayers arranged in the form of cochleate cylinders or lamellar sheets, which melt at very high temperatures, above 100 °C in the case of phosphatidylserine (Ca^{2+} only) and phosphatidic acid but below 100 °C in the case of phosphatidylglycerol, phosphatidylethanolamine (at high pH), and dimyristoylphosphatidylserine (Mg^{2+} only) (Verkleij et al., 1974; Ververgaert et al., 1975; van Dijck et al., 1975, 1978; Jacobson & Papahadjopoulos, 1975; Papahadjopoulos et al., 1975; Harlos & Eibl, 1980a,b; Liao & Prestegard, 1981; Hauser & Shipley, 1983). Besides being the cause of isothermal phase transitions, this behavior of divalent cations may also be involved in fusion (Papahadjopoulos et al., 1977).

The complex of synthetic forms of phosphatidylglycerol (PG)[1] with divalent cations undergoes metastable phase behavior at cation to lipid mole ratios greater than 0.5:1 (Ververgaert et al., 1975; van Dijck et al., 1975; Sacré et al., 1979; Fleming & Keough, 1983). The metastable phase melts at a temperature near that of the protonated form of the lipid. It then undergoes an exothermic transition to a stable state which melts with a greater enthalpy at 65–97 °C, depending on the cation and chain length. The accessibility of the phase transition of the stable state of PG below 100 °C makes this a useful lipid with which to study the structure of the metastable and stable states and the mechanism of conversion beween them. The stable state has been shown to be dehydrated and crystalline-like while the metastable phase is in the form of hydrated bilayers by X-ray diffraction (Harlos & Eibl, 1980a) and ^{31}P NMR spectroscopy (Cullis & de Kruijff, 1976; Farren & Cullis, 1980).

In their study of the effect of divalent cations on bovine brain phosphatidylserine (PS), Portis et al. (1979) suggested that the stable dehydrated state of the Ca^{2+} complex of PS is due to formation of a "trans" complex in which lipids in adjacent bilayers are bridged while complexes melting at a lower temperature (such as Mg^{2+}–PS) are due to a "cis" complex in which only adjacent molecules in the same bilayer are bridged. However, PS has not been observed to undergo metastable phase behavior. Copeland & Andersen (1981, 1982) have developed a statistical mechanical theory which attempts to account for the effects of divalent cations on lipid phase transitions including the metastable phase behavior of the PG complex. Making use of experimental data in the literature, they invoke cis-type bridging in the stable state but not the metastable or liquid-crystalline states to account for the metastability and the transition temperatures of the metastable and stable states. However, they did not take into account the close contact of bilayers in the stable state which appears to be necessary to explain the X-ray diffraction, freeze–fracture, and ^{31}P NMR results and cannot explain the fact that the stable phase only occurs at bound ratios of cation to lipid of 0.5:1. Furthermore, certain other features of the

† From the Research Institute, The Hospital for Sick Children, and The Department of Clinical Biochemistry, University of Toronto, Toronto, Ontario, Canada M5G 1X8. *Received March 29, 1983.* This investigation was supported by the Medical Research Council of Canada and by a Career Development Award from the Multiple Sclerosis Society of Canada to J.M.B.

[1] Abbreviations: DLPG, dilauroylphosphatidylglycerol; DMPG, dimyristoylphosphatidylglycerol; DPPG, dipalmitoylphosphatidylglycerol; DSPG, distearoylphosphatidylglycerol; DTPG, ditetradecylphosphatidylglycerol; PG, phosphatidylglycerol; PS, phosphatidylserine; DSC, differential scanning calorimetry; EPR, electron paramagnetic resonance; EDTA, ethylenediaminetetraacetic acid; Hepes, *N*-(2-hydroxyethyl)piperazine-*N*′-2-ethanesulfonic acid.

0006-2960/83/0422-5425$01.50/0

phenomenon presented in the present report cannot be entirely accounted for by this theory. In the present study, the effect of divalent and monovalent cation concentrations and the effect of heating and cooling rates on the metastable phase behavior of PG are examined. Also, changes in the binding of a divalent cation, Mn^{2+}, to the metastable, stable, and liquid-crystalline states of the Mn^{2+}–PG complex are determined from the EPR spectrum of Mn^{2+}, and a model is presented to account for the behavior of these lipid–divalent cation complexes.

Materials and Methods

Dipalmitoylphosphatidylglycerol (DPPG) was purchased from Supelco (Bellefonte, PA), and distearoylphosphatidylglycerol (DSPG) was purchased from Avanti (Birmingham, AL) and was washed with 0.1 M EDTA (Bligh & Dyer, 1959) to remove divalent cations. Dimyristoylphosphatidylglycerol (DMPG) was prepared enzymatically from dimyristoylphosphatidylcholine (from Sigma) by the method of Papahadjopoulos et al. (1973). All were chromatographically pure and melted at the correct temperatures for the Na^+ salt forms. $MgCl_2 \cdot 6H_2O$ and $CaCl_2 \cdot 2H_2O$ were from Fisher, and $MnCl_2 \cdot 4H_2O$ was from Sigma.

Preparation of Vesicles. The lipid (generally 1 mg) was dispersed at 45 °C by vortex shaking in Hepes buffer (2 mM at pH 7.4 containing the desired concentration of NaCl as specified in the text). An aliquot of 0.1 M $MgCl_2$, $CaCl_2$, or $MnCl_2$ solution prepared in the same buffer was then added in order to achieve the divalent cation concentration and lipid to cation mole ratio specified in the text; the sample was vortexed at 90–100 °C and then centrifuged 5 min in an Eppendorf microcentrifuge. The wet pellet was loaded into an aluminum DSC pan for calorimetry.

Differential Scanning Calorimetry. Samples were run on a Perkin-Elmer DSC-2 at heating or cooling rates of 1.25–10 °C/min. The temperature of maximal excess heat capacity was defined as the phase transition temperature (T_m). For the Ca^{2+} and Mg^{2+} samples, enthalpy determinations were made as described earlier (Boggs & Moscarello, 1978) except that the pans were opened by squeezing with forceps, dropping into a test tube containing 1 mL of chloroform–methanol (2:1), and sonicating by placing the tubes in a bath sonicator for a few minutes. The amount of lipid in the pans was determined by phosphorus analysis by a modified Bartlett (1959) procedure.

Enthalpy measurements of peak 1 of the Mg^{2+} complexes were obtained in the presence of 0.0125 M Mg^{2+}–0.02 M Na^+ by scanning from 17 °C at a heating rate of 10 °C/min. The maximum enthalpy of peak 2 of the Mg^{2+} complexes of DMPG, DPPG, and DSPG was obtained by scanning from 17 °C at 10 °C/min to 35, 55, and 64 °C, respectively, incubating at that temperature for 30 min, then cooling back to 17 °C, and reheating at a rate of 10 °C/min. The maximum enthalpy of peak 4 of the Ca^{2+} complexes of DMPG, DPPG, and DSPG was obtained by scanning from 17 °C at 10 °C/min to 75, 79, and 85 °C, respectively, incubating at that temperature for 30 min, cooling back to 17 °C, and reheating at a rate of 10 °C/min. In the case of the Mn^{2+} samples, the sample pans were not opened for lipid determination. However, the areas of the peaks in the DSC scans were determined by using a Perkin-Elmer data station and expressed as a percentage of the maximum area found for the melting transition of state B. The maximum area of peak 3 of the Mn^{2+} complex of DPPG was determined by scanning from 17 °C/min to 70 °C and incubating at 70 °C for 30 min. Unless otherwise noted, all cooling rates in between heating scans were 20–40 °C/min.

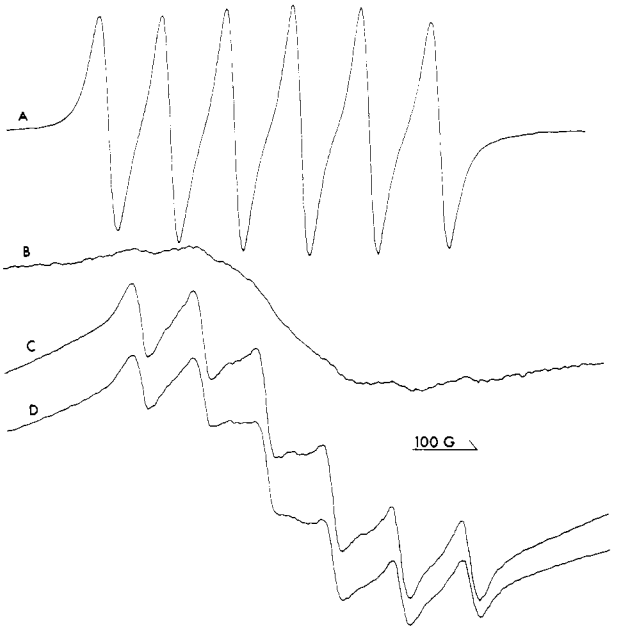

FIGURE 1: EPR spectra of Mn^{2+} at 20 °C (A) free in solution, (B) bound to DPPG at a bulk ratio of 0.4:1, (C) bound to DPPG in state A at a bulk ratio of 0.5:1, and (D) the same as in (C) but after conversion to state B by incubation at 64 °C. In spectra B–D, the pellet sample is placed in the center of the cavity so that the volume ratio of the lipid to the aqueous phase is high.

Electron Spin Resonance. Samples were taken up in 50-μL borosilicate glass micropipets (from Fisher) for EPR measurement of the signal due to Mn^{2+} free in solution. The spectrum of Mn^{2+} in the samples was measured on a Varian E-104B EPR spectrometer equipped with a variable temperature controller and compared to that of a standard solution measured at the same temperature.

The spectrum of either a homogeneous suspension of the vesicles, the supernatants from the pelleted samples, or the wet pellet itself was measured at different temperatures as described in the text. The cooling rate within the cavity of the spectrometer was 20–25 °C/min. Mn^{2+} free in solution gives a sharp six-line spectrum as shown in Figure 1A. The height of the lines is proportional to the concentration. Mn^{2+} bound to the lipid gives an exchange-broadened spectrum of greatly reduced intensity (as shown in Figure 1B) which does not interfere with the much more intense signal of Mn^{2+} free in solution (Galla & Sackmann, 1975; Puskin, 1977; Boggs et al., 1981a), provided the vesicle concentration is low. If the lipid concentration is high as when the pellet is used, the signal due to free Mn^{2+} can be distinguished from the signal due to bound Mn^{2+} as shown in Figure 1C,D, and relative changes in the amount of free Mn^{2+} can be determined from changes in the height of one of the peaks. The most low-field peak was chosen. When using a homogeneous suspension or the supernatant from the vesicles, it was possible to determine the amount of free Mn^{2+} from the following expression:

$$\mu\text{mol of free } Mn^{2+} = (h_{sa}/h_{st})(\mu\text{mol of total } Mn^{2+})$$

where h_{sa} and h_{st} are the heights of the EPR spectrum of the sample and standard solutions, respectively.

The molar ratio of Mn^{2+} bound to DPPG is determined from

$$\text{bound } Mn^{2+}\text{:DPPG} = \frac{\mu\text{mol of total } Mn^{2+} - \mu\text{mol of free } Mn^{2+}}{\mu\text{mol of total DPPG}}$$

The DPPG concentration was determined by phosphorus

Table I: Phase Transition Temperatures of Different Forms of DPPG

	PG:cation mole ratio	heat[a] T_1	T_2	T_3	T_4	cool[b] T_f
DPPG-Na^+ (pH 7.4)		41.7				39.3
DPPG-H (pH 1.1)		63.3				60.3
DPPG-Mn^{2+}	1:0.6	61.9	83.7	87.7		57.8-60.4[c]
DPPG-Mg^{2+}	1:0.4	50.0				
DPPG-Mg^{2+}	1:0.5	51.0				
DPPG-Mg^{2+}	1:1	54.2	78.7			53
DPPG-Ca^{2+}	1:0.2	50-54				
DPPG-Ca^{2+}	1:0.3	55.7				
DPPG-Ca^{2+}	1:0.4	58				
DPPG-Ca^{2+}	1:0.5	61.9	82.8	84.6	91.6	56.7-75.6[c]

[a] Determined from heating scans at 10 °C/min. [b] Determined from cooling scans at 1.25 °C/min. [c] Depends on cation concentration and cooling rate.

analysis to an accuracy of ±5%.

When measurements were made on the pellet, the free Mn^{2+} concentration or bound Mn^{2+}:DPPG molar ratio could not be quantitated since the pellet volume took up a substantial but unknown proportion of the sample volume and it was not possible to measure the signal due to the same volume of the standard solution. However, relative changes in the free Mn^{2+} concentration could be determined from changes in the peak height, and the measurements could be corrected for the temperature dependence of the spectrum by dividing the height of the sample spectrum, h_{sa}, by the height of the standard solution spectrum, h_{st}, measured at the same temperature. This gave reasonable values except at very low temperatures where the height of the spectrum due to free Mn^{2+} in the sample is low and probably distorted by the exchange-broadened spectrum of bound Mn^{2+}; i.e., h_{sa}/h_{st} was similar at all temperatures above 20 °C under conditions where no change in free Mn^{2+} concentration occurs, but at temperatures below 20 °C, h_{sa}/h_{st} increased.

Results

The effect of divalent cations on PG depends on the mole ratio of cation to lipid as well as on the cation concentration. Increasing amounts of Ca^{2+} and Mg^{2+} at ratios less than 0.5:1 gradually increase the phase transition temperature from that of the sodium salt form to a value approaching but never reaching that of the protonated form, 63.3 °C, as shown for DPPG in Table I and in agreement with results presented by van Dijck et al. (1975) and Papahadjopoulos (1977). A transition at a temperature higher than 63.3 °C is never observed at ratios less than 0.5:1. When the ratio is close to or equal to 0.5:1 in the case of Ca^{2+} and Mn^{2+} or greater than 0.5:1 in the case of Mg^{2+} (this is the bulk ratio of cation added, and it is likely that the amount of Mg^{2+} bound is also in the ratio 0.5:1), there is a pronounced change in the thermal behavior as shown in Figure 2. In the case of Mg^{2+}, the endothermic transition at 54 °C (T_1) is followed by an exothermic transition and then another endothermic transition at 79 °C (T_2). In the case of Ca^{2+} and Mn^{2+}, there may be an endothermic transition (Figure 2e), an exothermic transition (Figure 2d,f), or both (Figure 2g) at 50–68 °C. In the case of Ca^{2+}, the first endothermic and exothermic transitions are followed by three more endothermic transitions at 82–92 °C (T_2, T_3, and T_4) (Table I). The third and fourth endothermic transitions of the Ca^{2+} complex are also preceded by exothermic transitions, indicating that all the phases giving peaks 1, 2, and 3 are metastable. This is not apparent in Figure 2

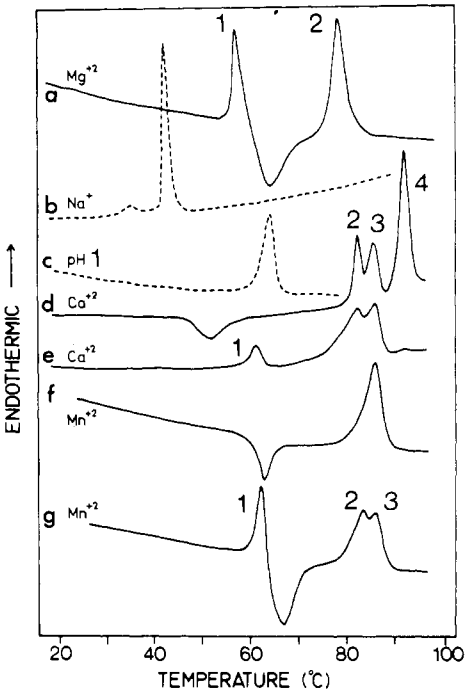

FIGURE 2: DSC heating thermograms of DPPG in the presence of (a) 0.0125 M Mg^{2+}, (b) 0.1 M Na^+, pH 7.4, (c) 0.1 M Na^+, pH 1, (d and e) 0.0125 M Ca^{2+}, and (f and g) 0.0025 M Mn^{2+}. Thermograms a, e, and g were heated from 20 °C while the rest were heated from 0 °C. Heating rate, 10 °C/min. Peaks 1 and 2 of the Mg^{2+} complex, peaks 1–4 of the Ca^{2+} complex, and peaks 1–3 of the Mn^{2+} complex are indicated. Different amounts of lipid were present in the pans so the relative peak areas cannot be compared except for the pairs (d), (e) and (f), (g) where the same sample was scanned from different temperatures. The sensitivity settings in millicalories per second were (a) 0.5, (b) 1.0, (c) 0.8, (d and e) 1.0, and (f and g) 0.8.

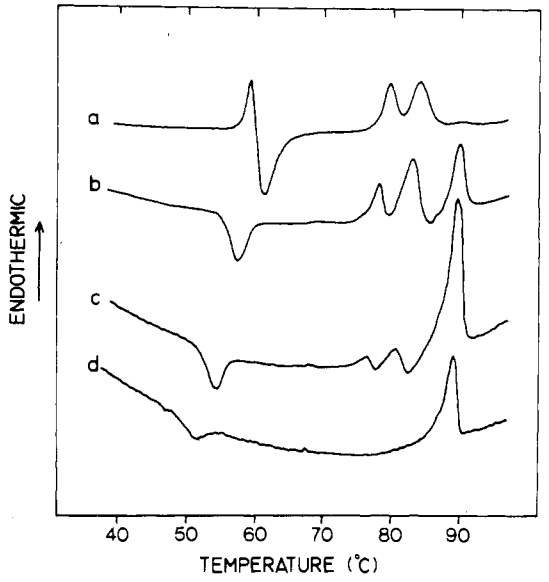

FIGURE 3: Effect of heating rate on DSC thermograms scanned from 17 °C of Ca^{2+}–DPPG in 0.0125 M Ca^{2+} and 0.02 M Na^+, PG:Ca^{2+} = 1:3.6. The heating rates were (a) 10, (b) 5, (c) 2.5, and (d) 1.25 °C/min. The sensitivity settings in millicalories per second were (a) 5, (b) 2, and (c and d) 1.

but was observed in some scans (see Figure 3c). In the presence of Mn^{2+}, there were at most two high-temperature endothermic transitions, T_2 and T_3. Note that for all three cations, even at ratios greater than 0.5:1, the temperature of peak 1 is less than 63.3 °C (Figure 2c and Table I), although T_1 is higher for the Ca^{2+} and Mn^{2+} complexes than for the Mg^{2+} complex.

The hydrated metastable phase giving rise to peak 1 is defined as state A, the dehydrated (or partially dehydrated) stable phase giving rise to peak 2 in the case of Mg^{2+}, peak 4 in the case of Ca^{2+}, and peak 3 in the case of Mn^{2+} as state B, and the highest temperature liquid-crystalline phase as state C. Similar notation was also used for the phases of Ca^{2+}–DTPG (Harlos & Eibl, 1980a) and the complex of DPPG with myelin basic protein, which also has metastable phase behavior (Boggs et al., 1981b). The other metastable phases giving rise to peaks 2 and 3 in the case of Ca^{2+} are defined as B′ and B″, respectively, while that giving rise to peak 2 in the case of Mn^{2+} is defined as state B′. These phases may be due to varying degrees of dehydration.

The behavior reported here for the Ca^{2+} complex is somewhat different from that reported by others for DLPG and DTPG, for which only peak 1 and one of the high-temperature peaks were observed (Sacrê et al., 1979; Harlos & Eibl, 1980a), and DMPG and DPPG for which only peaks 2, 3, and 4 were observed (van Dijck et al., 1975, 1978). Fleming & Keough (1981, 1983), however, have reported four transitions for DLPG. This discrepancy between different reports is at least partly due to the fact that the actual appearance of the scans and the relative heights of all the transitions depend on the experimental conditions and the heating rate. This indicates that the rate of the exothermic process depends on these factors which, as will be shown below, include the divalent and monovalent cation concentrations and the temperature to which the sample is cooled before the heating scan.

Effect of Initial Temperature and Heating Rate. Figure 2d,f shows the effect of cooling to 0 °C rather than to 20 °C as in Figure 2e,g for the Ca^{2+} and Mn^{2+} complexes. Cooling to the lower temperature eliminates the first endothermic transition, lowers the temperature of the exothermic transition, and increases the height of the final peak (with complete elimination of peak 2 in the case of Mn^{2+}), indicating that it causes an increase in the rate of the transition to state B. Although the first endothermic transition is absent in Figure 2d,f at the heating rate used, 10 °C/min, it is observed at a faster heating rate, indicating that the sample was also initially in the metastable state when cooled to 0 °C as when cooled to 20 °C.

The effect of the heating rate on the Ca^{2+} complex of DPPG is shown in Figure 3. As the heating rate decreases, peak 1 disappears, and the first exothermic transition becomes broader and is shifted to lower temperatures. The relative height of peak 2 also decreases; the height of peak 3 increases and then decreases as the height of peak 4 increases. The temperatures of peaks 2, 3, and 4 were constant with changes in the heating rate. The continuous decrease in temperature and broadening of the exothermic transition with a decrease in the heating rate indicates that the exothermic process occurs slowly over a wide temperature range, but the rate of the process is faster at higher temperatures. A decrease in the heating rate had a similar effect on the thermograms of the Mg^{2+} and Mn^{2+} complexes except that for the Mg^{2+} complex the first endothermic transition never completely disappeared and the temperature of the exothermic transition did not decrease as much as for the Ca^{2+} and Mn^{2+} complexes (not shown).[2]

Effect of Fatty Acid Chain Length. The samples could be completely converted to state B by incubation at or near the temperature of the exothermic transition, as described under Materials and Methods, in order to determine the maximum enthalpy of the final transition. X-ray diffraction measurements have shown that this procedure allowed conversion of Ca^{2+}–DTPG to state B (Harlos & Eibl, 1980a). After this treatment, the subsequent thermogram showed only a single peak at T_2 in the case of Mg^{2+}, T_4 in the case of Ca^{2+}, and T_3 in the case of Mn^{2+} (not shown).[2] Therefore, the maximum enthalpy of the final transition is assumed to be the enthalpy of state B, ΔH_B. It was necessary to heat at a rate of 10 °C/min or less up to 72 °C in order to obtain complete conversion to state B, indicating that the sample must go completely into state B′ before it can go into states B″ or B. No conditions were found which converted the sample completely and only into states B′ and B″. The enthalpy of state A of the Mg^{2+} complex could be determined by choosing the experimental conditions, as described under Materials and Methods, such that the rate of conversion to state B was sufficiently slow that only a single endothermic peak at T_1 was observed on scanning at 10 °C/min. However, the enthalpy of state A of the Ca^{2+} and Mn^{2+} complexes could not be determined as the rate of the exothermic process was too fast to permit the sample to remain in state A during the scan under any of the experimental conditions tried. The effect of fatty acid chain length on the transition temperatures and enthalpies of the Mg^{2+} and Ca^{2+} complexes was determined.

The behavior of DMPG and DSPG with Mg^{2+} and Ca^{2+} was similar to that described for DPPG. The T_m and ΔH values are given in Table II along with values reported in the literature for DLPG and DTPG. The temperature intervals between peaks 1 and 2 for the Mg^{2+}–PG complexes and between peak 1 and the other three peaks for the Ca^{2+}–PG complexes decreased with increase in chain length. As shown in Figure 4, T_1 of the divalent cation complexes shows a strong,

Table II: Effect of Mg^{2+} and Ca^{2+} on the Phase Transition Temperatures and Enthalpies of the Metastable and Stable States of Synthetic Species of PG with Varying Fatty Acid Chain Lengths[a]

	Mg^{2+}				
	T_1 (°C)	ΔH_1 (kcal/mol)[b]	T_2 (°C)	ΔH_2 (kcal/mol)	$\Delta H_2/\Delta H_1$
DLPG	20[c]	5–5.5[c]	72[c]	10[c]	1.82–2
DMPG	36	5.4 ± 0.3	65	9.9 ± 0.3	1.82
DPPG	54.2	8.0 ± 0.4	78.7	13.6 ± 0.9	1.70
DSPG	66.1	8.7 ± 0.3	81	13.6 ± 0.9	1.56

	Ca^{2+}				
	T_1 (°C)[h]	T_2 (°C)	T_3 (°C)	T_4 (°C)	ΔH_4 (kcal/mol)
DLPG	27[d] 19–22[c,e]	58[d]	73[d] 67–72[c,e]	82[d]	10[c]
DMPG	41	70	76.5	84.2	10.9 ± 1.5
DPPG	61.9	82.8	84.6	91.6	11.3 ± 1.0
DSPG	68	86	89	97.2	12.6 ± 1.2
DTPG	46[f]	61, 63[f,g]		81–83[f]	9[f]

[a] At a heating rate of 10 °C/min. [b] Of the Na^+ salt forms, we have determined ΔH of DPPG only. It is 8.3 ± 0.7 kcal/mol (Boggs et al., 1981b), similar to that reported elsewhere and to that of peak 1 of Mg^{2+}-DPPG. However, the values for ΔH_1 of DMPG and DSPG are lower than those reported elsewhere for the Na^+ salt form. This may be due to some systematic error in the determination of the amount of lipid or a difference in calibration of the instrument. However, the ratio of the enthalpies of peaks 1 and 2 depends only on the ratio of peak areas and can be determined more accurately than the enthalpy. [c] Ververgaert et al. (1975). [d] Fleming & Keough (1983). [e] Sacré et al. (1979). [f] Harlos & Eibl (1980a). [g] Small, broad peaks. [h] ΔH_1 of the Ca^{2+} complex could not be determined because the sample converted to state B too rapidly. van Dijck et al. (1975) determined ΔH_1 of the Ca^{2+} complex of DLPG and DMPG by using Ca^{2+}:PG ratios of less than 0.5:1 and found it to be similar to the enthalpy of the transition of the Na^+ salt forms and of ΔH_1 of the Mg^{2+} complexes.

[2] Data described in the text are available upon request from J.M.B.

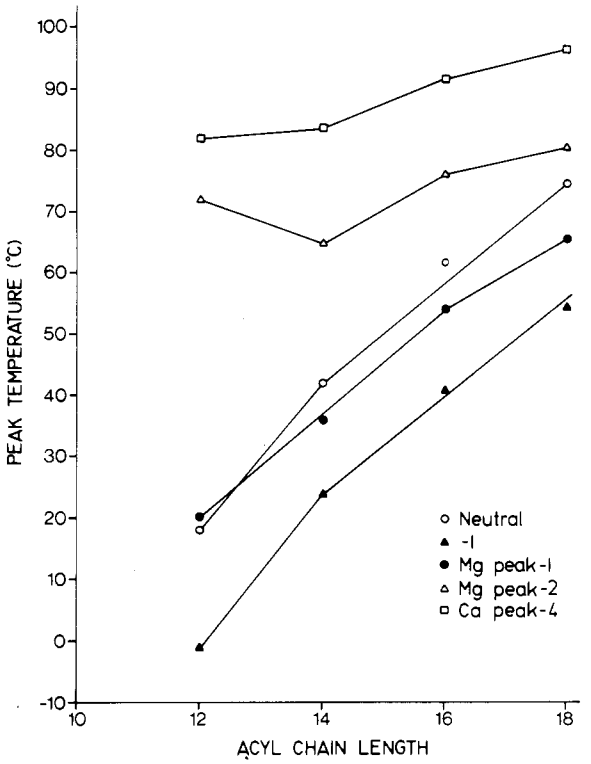

FIGURE 4: Dependence of phase transition temperature of PG on fatty acid chain length (number of carbons) for the Na^+ salt form (▲), the protonated form (○), peak 1 (●) and peak 2 (△) of the Mg^{2+} complex, and peak 4 (□) of the Ca^{2+} complex. Data for DLPG are from Sacré et al. (1979) for the Na^+ salt and protonated forms, from Ververgaert et al. (1975) for the Mg^{2+} complex, and from Fleming & Keough (1981) for the Ca^{2+} complex. Data for the protonated forms of DSPG and DMPG are from Findlay & Barton (1978) and van Dijck et al. (1978), respectively. The chain length dependence of peak 1 of the Ca^{2+} complex was similar to that of the Mg^{2+} complex while that of peaks 2 and 3 of the Ca^{2+} complex was similar to that of peak 4 and is not shown.

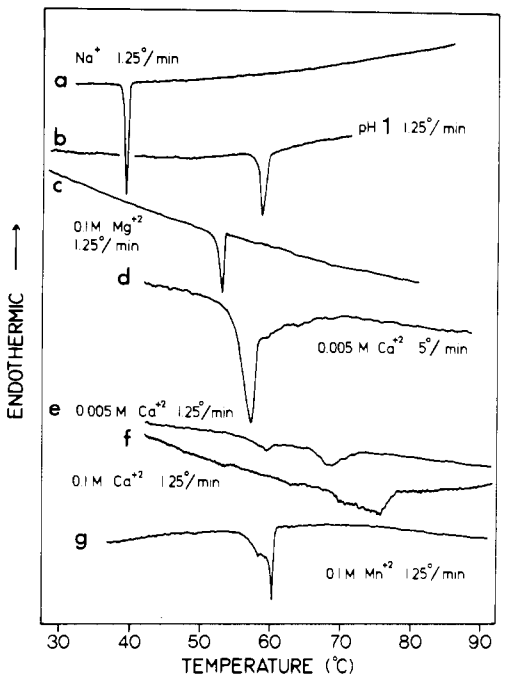

FIGURE 5: DSC cooling thermograms of DPPG in the presence of (a) 0.1 M Na^+, pH 7.4, (b) 0.1 M Na^+, pH 1, (c) 0.1 M Mg^{2+}, (d and e) 0.005 M Ca^{2+}, (f) 0.1 M Ca^{2+}, and (g) 0.1 M Mn^{2+}. Cooling rates are 1.25 °C/min for all except (d) which is 5 °C/min. Different amounts of lipid were present in the pans so the relative peak areas cannot be compared except for (d) and (e) where the same sample was scanned at different rates. The sensitivity settings in millicalories per second were (a) 0.5, (b–e) 0.3, (f) 0.2, and (g) 0.3.

almost linear dependence on fatty acid chain length similar to that of the Na^+ salt and protonated forms. However, the T_m of peaks 2, 3, and 4 of the divalent cation complexes shows much less dependence on chain length.

The reported enthalpies of the Na^+ salt form of PG also depend linearly on fatty acid chain length (Findlay & Barton, 1978; Ververgaert et al., 1975; van Dijck et al., 1975, 1978). The enthalpy of state A of the Mg^{2+} and Ca^{2+} complexes is close to that of the Na^+ salt form, but the enthalpy of state B is much greater as reported by Ververgaert et al. (1975) and van Dijck et al. (1975, 1978) (Table II). However, while this group found that the enthalpy of state B was more than double that of state A, particularly for the Ca^{2+} complexes of DMPG and DPPG, our data shown in Table II indicate that the enthalpy of state B is less than that. Harlos & Eibl (1980a) found that the enthalpy of state B of the Ca^{2+}–DTPG was only 1.8 times that of state A, which is more consistent with our values. Table II shows further that the ratio of enthalpies of peak 2 to peak 1 of the Mg^{2+} complex decreases with fatty acid chain length. Thus, as for the transition temperature, there appears to be less dependence of the enthalpy of state B on fatty acid chain length than that of state A and little difference between the enthalpy values of state B of the Mg^{2+} and Ca^{2+} complexes.

Effect of Cooling Rate. On cooling, at all rates between 10 and 1.25 °C/min, the Mg^{2+} complex of DPPG shows only a single sharp transition at 53 °C (Figure 5c, Table I), 7.3 °C below the T_m of the protonated form (Figure 5b) and with an enthalpy similar to that of state A on heating or about 60% of that of state B. The excess enthalpy of the exothermic transition on heating (difference between the heat released during the exothermic transition and that absorbed during the first endothermic transition) was about 22% of that of state B. Thus, about 82% of the enthalpy of state B of the Mg^{2+} complex could be accounted for. However, in the case of Ca^{2+}, the temperature and enthalpy of the freezing transition depend on the cooling rate as shown in Figure 5d,e and Table III. When the sample is cooled at a fast rate (10 °C/min), it freezes at 57 °C with a relatively sharp transition (Figure 5d). Cooling at a slower rate allows the sample to freeze at a higher temperature, as high as 75.6 °C (Figure 5f), well above the T_m of the protonated form but still below T_2, T_3, and T_4 of

Table III: Effect of Cooling Rate on the Enthalpy of the Freezing Transition (ΔH_f) and the Enthalpy of the Exothermic Transition of the Subsequent Heating Scan (ΔH_{ex}) of the Ca^{2+}–DPPG Complex[a]

sample	cooling rate (°C/min)	ΔH_f (% of ΔH_B)	ΔH_{ex} (% of ΔH_B)
1	20–40		22
	10	41	18
	5	55	8
	2.5	63	4
	1.25	65	0
2	20–40		23
	5	50	11
	2.5	73	low
	1.25	85	0

[a] Representative samples, 0.001 M Ca^{2+}, PG:Ca^{2+} 1:0.74, heating rate 10 °C/min. The signal to noise ratio decreases and the base-line curvature or slope increases at slower heating and cooling rates so that the peak area cannot be measured as accurately. The difference in results between samples 1 and 2 illustrates the typical spread in the data found when measuring the area of broad peaks from cooling scans such as those shown in Figure 5e,f.

Table IV: Effect of Incubation at Different Temperatures on the Enthalpies of the Freezing Transition (ΔH_f) and the Exothermic Transition (ΔH_{ex}) of the Subsequent Heating Scan for the Mn^{2+}-DPPG Complex[a]

treatment	incubation temp (°C)	ΔH_f[b] (% of ΔH_B)	ΔH_{ex}[c] (% of ΔH_B)
sample 1[d]			
100 → 0 °C	none	44	29
100 → 72 → 0 °C	72	45	26
100 → 72 → 82 → 0 °C	72	31	16
100 → 62 → 82 → 0 °C	62	0	0
sample 2[d]			
100 → 0 °C	none		24
100 → 72 → 0 °C	72		19
100 → 57 → 0 °C	57		12
100 → 67 → 82 → 0 °C	67		0
100 → 57 → 82 → 0 °C	57		0
100 → 47 → 82 → 0 °C	47		17
sample 3[e]			
100 → 0 °C	none		24
100 → 57 → 0 °C	57		4

[a] Samples were cooled rapidly from 100 °C to incubation temperature, held there for 20 min, and then cooled rapidly from that temperature, or a higher temperature, to 0 °C. Under these conditions, no endothermic transition at T_1 occurred. [b] Cooling rate 1.25 °C/min. [c] Heating rate 10 °C/min, subsequent heating scan. [d] 0.001 M Mn^{2+}; bulk ratio Mn^{2+}:PG, 0.6:1. [e] 0.0025 M Mn^{2+}; bulk ratio Mn^{2+}:PG, 0.6:1.

the three endothermic transitions seen on heating. The enthalpy of the transition on cooling, ΔH_f, increased from about 41% to a maximum of 85% of that of state B, (ΔH_B), with a decrease in the cooling rate from 10 to 1.25 °C/min (Table III).

Furthermore, the appearance of the subsequent heating scan also depends on the rate at which the sample had been cooled. After fast cooling, the enthalpy of the exothermic transition, ΔH_{ex}, is 22–25% of ΔH_B. As the cooling rate decreases, and the enthalpy of ΔH_f increases, ΔH_{ex} of the subsequent heating scan decreases and ultimately disappears (Table III). Loss of the exothermic transition after slow cooling was also reported for Ca^{2+}–DLPG by Sacrē et al. (1979). Thus, as for the Mg^{2+} complex, only about 85% of the enthalpy of state B can be accounted for. The remaining portion of ΔH_B must be absorbed noncooperatively either on cooling or on heating at temperatures above T_{ex}. The ratio of peaks 2, 3, and 4 in the subsequent heating scan also depends on the cooling rate. Surprisingly, slow cooling caused peak 3, the transition of state B″, to be increased at the expense of peaks 2 and 4 (not shown).[2] Thus, during slow cooling, the sample refreezes into state B′, or B″ rather than state A. If a slower heating rate is used on the subsequent heating scan, the height of peak 4 increases as it did after rapid cooling, but slow cooling evidently stabilizes state B″ relative to B. The maximum enthalpy of peak 3 observed when peaks 2 and 4 were minor components of the scan was comparable to ΔH_B. Thus, states B″ and B probably have similar enthalpies.

The Mn^{2+} complex refroze at a temperature betwen 58 and 60 °C on cooling even at a cooling rate as slow as 1.25 °C/min (Figure 5g). The enthalpy of the freezing transition, ΔH_f, was about half of ΔH_B while ΔH_{ex} of the subsequent heating scan was about 25% of ΔH_B (Table IV). It was not practical to cool more slowly than 1.25 °C/min. To determine if the Mn^{2+} sample could freeze at a temperature higher than 60 °C and the effect of this on the subsequent heating scan, the sample was cooled rapidly to different temperatures and incubated at that temperature for 20 min. A cooling scan at 1.25 °C/min from the incubation temperature, or a slightly higher temperature, and a heating scan at 10 °C/min were then obtained. ΔH_f of the cooling scan and ΔH_{ex} of the subsequent heating scan are shown in Table IV. Cooling of sample 1 to 62 °C and incubating at that temperature for 20 min completely eliminates the freezing transition, as expected since this is close to the temperature of the freezing transition observed on scanning (Figure 5g). However, it also eliminated the exothermic transition on the subsequent heating scan which did not happen after a cooling scan at 1.25 °C/min. Only peak 3 was observed on the subsequent heating scan, indicating that if the sample was given sufficient time at 62 °C it refroze into state B while it refroze into state A after cooling at a rate of 1.25 °C/min or greater.

In order to perform the cooling scan after incubation, it was necessary to heat the sample up to some temperature above the freezing temperature of 60 °C and cool from there. This was found to increase the percent conversion to state B during cooling as can be seen by comparing ΔH_{ex} after incubation at 57 °C and cooling directly to 0 °C to that after incubation at 57 °C and heating to 82 °C before cooling to 0 °C (sample 2, Table IV). However, at a higher Mn^{2+} concentration, used for sample 3 (Table IV), it was not necessary to heat to 82 °C after incubation at 57 °C for 20 min to eliminate ΔH_{ex} on the next heating scan. Incubation temperatures higher than 72 °C or lower than 47 °C were found to be much less effective at eliminating ΔH_f or ΔH_{ex}. The effectiveness of temperatures between 60 and 72 °C indicates that the freezing transition can occur in this range, if given sufficient time, as observed for the Ca^{2+} complex, even though no transition is observed above 60 °C by cooling as slowly as 1.25 °C/min.

Effect of Divalent Cation Concentration. The effect of divalent cation concentration (at constant ratios greater than 0.5:1) on the rate of conversion of state A to state B was examined by determining the slowest heating rate which allowed maximum conversion to state B. This was done by comparing the height or area of peak 2 for the Mg^{2+} complex, peak 4 for the Ca^{2+} complex, and peak 3 for the Mn^{2+} complex, at different heating rates, to the height or area expected if the sample is completely converted to state B, as described previously (Boggs et al., 1982). The maximum height after complete conversion to state B was determined after incubation of the sample as for the enthalpy measurement. The expected height at each heating rate was obtained by multiplying the maximum height from a 10 °C/min scan by a correction factor to account for the normal decrease in height which occurs at lower heating rates (since the units of the ordinate are millicalories per second).

As shown in Table V, the rate of conversion to state B was found to depend on Mg^{2+} concentration over the range 0.001–0.01 M and on Mn^{2+} concentration over the range 0.0005–0.0025 M but not on Ca^{2+} concentration over the range 0.0002–0.01 M. However an increase in rate was found at very high Ca^{2+} concentrations above 0.1 M. At 0.001 M Mg^{2+}, the rate was so slow that no second peak was observed even at the slowest heating rate used, 1.25 °C/min, nor after incubation at 55 °C for 90 min. At 0.0025 M Mg^{2+}, there was a small second peak present, but it did not increase substantially after slow heating or incubation. The rate was much faster at 0.003 M and higher Mg^{2+} concentrations, allowing estimation of the percent conversion at different heating rates as shown in Table V. Similar results were obtained for the Mn^{2+} sample.

For the Ca^{2+} complex, the rate of formation of the stable state on cooling depended on Ca^{2+} concentration even though the rate on heating did not. At concentrations below 0.001 M, the freezing transition occurred at 55 °C, even at a slow

Table V: Effect of Divalent Cation Concentration on the Percent Conversion of DPPG to State B[a]

DSC heating rate (°C/min)	Mg^{2+} (DPPG:Mg^{2+} = 1:0.74) cation concn (M) 0.003[b]	0.0035	0.005	0.01
20	0		1.6	1.4
10	53	67.3	73.6	87.0
5	81	91.2	100	100
2.5	100	100	100	100
1.25	100	100	100	100

DSC heating rate (°C/min)	Ca^{2+} (DPPG:Ca^{2+} = 1:0.74) cation concn (M) 0.0002	0.0025	0.01	0.1	1.0
20		2.6	2.7	2	18.3
10	53	58	65	100	100
5	100	100	100	100	100
2.5	100	100	100	100	100
1.25	100	100	100	100	100

DSC heating rate (°C/min)	Mn^{2+} (DPPG:Mn^{2+} = 1:0.6) cation concn (M) 0.0005	0.0025
20	3.4	64.6
10	7.1	88.2
5	8.6	100
2.5	36.2	100
1.25	37.3	100

[a] Ca^{2+} and Mg^{2+} samples scanned from 0 °C, Mn^{2+} sample scanned from 27 °C. Cooled 20–40 °C/min between heating scans. [b] At lower Mg^{2+} concentrations, little or none of the sample was converted to state B as discussed in the text.

Table VI: Effect of Na^+ Concentration on the Percent Conversion of the DPPG–Divalent Cation Complex to State B[a]

DSC heating rate (°C/min)	Mg^{2+} Complex (0.01 M Mg^{2+}, DPPG:Mg^{2+} 1:1.85) NaCl concn (M) 0	0.1	0.2[b]
20	1.5	0	0
10	81.1	0	0
5	100	74.4	42
2.5	100	100	77
1.25	100	100	100

DSC heating rate (°C/min)	Ca^{2+} Complex (0.0025 M Ca^{2+}, DPPG:Ca^{2+} 1:0.74) NaCl concn (M) 0	0.01	0.025	0.1[c]
20	2.6	0		0
10	58	68	39.6	11.7
5	100	100	100	32.1
2.5	100	100	100	74.3
1.25	100	100	100	100

DSC heating rate (°C/min)	Mn^{2+} Complex (0.001 M Mn^{2+}, DPPG:Mn^{2+} 1:0.74) NaCl concn (M) 0	0.025
10	100	20.7
5	100	29.4
2.5	100	45.0
1.25	100	45.3

[a] Ca^{2+} and Mg^{2+} samples scanned from 0 °C; Mn^{2+} sample scanned from 17 °C. Cooled 20–40 °C/min between heating scans. [b] At 0.5 M NaCl, none of the sample was converted to state B. [c] At 0.2 M NaCl, little conversion to state B occurred as discussed in the text.

cooling rate (1.25 °C/min) (not shown)[2], and the stable state was not formed on cooling as was evident from the subsequent heating scan. However, at 0.0025–0.005 M Ca^{2+}, the freezing transition occurred partially at 69 °C at this slow rate (Figure 5e). A further increase in Ca^{2+} concentration to 0.1 M caused the sample to freeze at 76 °C at this cooling rate (Figure 5f), and the subsequent heating scan showed that the sample refroze into the stable state. Mg^{2+} concentration had no effect on the temperature of the freezing transition up to 0.1 M Mg^{2+} and a lipid to Mg^{2+} mole ratio of 1:7.4. The freezing temperature increased slightly with an increase in Mn^{2+} concentration, but not above 60.4 °C at a cooling rate of 1.25 °C/min as described above. However, results for samples 2 and 3 in Table IV indicate that the rate of formation of the stable state on cooling does depend on the Mn^{2+} concentration since incubation at 57 °C for 20 min decreased ΔH_{ex} of the subsequent heating scan by a greater amount at 0.0025 M Mn^{2+} than at 0.001 M Mn^{2+}.

Effect of Monovalent Cation Concentration. An increasing concentration of monovalent cation (Na^+) decreased the rate of conversion to state B for the complexes of DPPG with all three divalent cations, as shown in Table VI; 25 mM NaCl had a substantial effect. In the presence of 500 mM NaCl, the rate for the Mg^{2+} complex was so slow that no second peak was observed even after incubation at 55 °C for 1 h. For the Ca^{2+} complex at 200 mM NaCl, a small peak at T_4 appeared at heating rates of 5 °C/min or less, indicating that conversion to state B occurred but at a slow rate. High Na^+ concentrations broadened the upper temperature transition as well as decreasing the height of peak 4 and the rate of conversion of the Ca^{2+} complex to state B. Instead of peaks 2 and 3, there was only a single endothermic transition at a temperature intermediate between T_2 and T_3 (not shown).[2] Increasing sodium concentration also decreased the temperature of the freezing transition on cooling at a given cooling rate, indicating that it decreased the rate of formation of the stable state on cooling. An increased concentration of Na^+ also broadened the freezing transition of the Mn^{2+} complex and shifted it to a slightly lower temperature.

Mn^{2+} Binding. Changes in the amount of bound and free Mn^{2+} after various sample treatments and at different temperatures were determined from the EPR spectrum of free Mn^{2+} as described under Materials and Methods. Puskin & Martin (1979) used this technique to measure the binding of Mn^{2+} to DPPG above and below its phase transition and showed that the association constant is 5 times greater in the gel phase than in the liquid-crystalline phase. However, the Mn^{2+} to lipid ratio in that study was chosen to be much less than 0.5:1, and thus the lipid phase transition temperature was not increased above that of the Na^+ salt form and there was no metastable phase behavior. In the present study, the Mn^{2+} to lipid ratio is close to 0.5:1, sufficient to induce metastable phase behavior, but not in great excess, which would make it difficult to detect small changes in the free Mn^{2+} concentration. The Mn^{2+}:DPPG bound ratio was only (0.46–0.49):1 at bulk ratios of (0.5–0.6):1 and became equal to 0.5:1 only at a bulk ratio of 1:1. However, DSC scans on the same samples as used for EPR studies at bulk ratios of (0.5–0.6):1 were similar to those shown in Figure 2f. At bulk ratios of less than 0.48:1 where the bound ratio was less than 0.46:1, the DSC scans showed that a portion of the lipid was not converted to state B under any conditions tried. Na^+ decreased the bound Mn^{2+}:PG ratio as expected (data not shown),[2] thus accounting for the decreased rate of conversion of state A to B in the presence of Na^+.

Changes in the bound Mn^{2+}:PG ratio at different temperatures were determined in several different ways. Each type of experiment was associated with certain problems. In one type of experiment, the EPR spectrum of a homogeneous suspension was measured at different temperatures. Data from

Table VII: Mole Ratio of Bound Mn^{2+} to DPPG in Different Phase States and after Various Sample Treatments

sample treatment	phase state	temp of measurement (°C)	bound Mn^{2+}:PG mole ratio	% difference between states B and C
		Experiment 1[a]		
after preparation	B	20	0.460	
	C	92	0.451	
92 → 20 °C	A	20	0.450	
92 → 20 → 52 °C for 37 min	B	20	0.457	1.9
		Experiment 2[b]		
95 → 4 → 70 °C for 1 h	B		0.486 ± 0.003	
95 °C for 15 min	C		0.475 ± 0.002	2.3 ± 0.5
		Experiment 3[b]		
95 → 4 °C	A		0.477 ± 0.004	
95 → 65 °C for 20 min	B		0.482 ± 0.0035	
95 → 4 → 65 °C for 20 min	B		0.484 ± 0.002	
95 → 37 → 65 °C for 20 min	B		0.482 ± 0.0035	
95 °C for 20 min	C		0.468 ± 0.001	3.2 ± 0.4

[a] Homogeneous suspension of Mn^{2+}-DPPG in a capillary tube measured at different temperatures in an EPR spectrometer. Bulk concentration of Mn^{2+} is 0.005 M, and bulk ratio of Mn^{2+}:PG is 0.5:1. [b] Samples were pelleted by centrifugation and then treated at different temperatures as indicated. Supernatants were then removed at 95 °C for the sample incubated at 95 °C or after cooling back to 4 °C for the other samples. Supernatants were measured at the same temperature as a standard Mn^{2+} solution. Bulk Mn^{2+} concentration and Mn^{2+}:PG ratio were 0.003 M and 1:0.6 for experiment 2 and 0.001 M and 1:0.6 for experiment 3, respectively. Data for experiment 2 are an average of four determinations while those of experiment 3 are an average of two determinations.

a representative sample in 0.005 M Mn^{2+} with ratio of bulk Mn^{2+} to lipid of 0.5:1 are shown in Table VII (experiment 1). At this bulk ratio, the ratio of Mn^{2+} bound to PG was found to be 0.460 in state B at 20 °C. In state C at 92 °C, the ratio of bound Mn^{2+} to PG had decreased to 0.451, a difference of 1.9%. On cooling back to 20 °C (at a rate of 20–25 °C/min), the sample is in the metastable state A, and the ratio is similar to that in state C, indicating that the Mn^{2+} had not rebound. After the sample was incubated at 52 °C for 37 min to convert it to state B, the bound Mn^{2+}:PG ratio had increased to 0.457, indicating that the Mn^{2+} became rebound at 52 °C. Once the sample had been taken through this series of temperature changes, it became aggregated and floated to the top of the aqueous phase in the capillary tube. A repeated increase in temperature to 92 °C did not cause any change in the EPR signal height, presumably because the Mn^{2+} dissociating from the lipid was not able to diffuse throughout all of the liquid in the capillary tube.

In another type of experiment, the sample was pelleted by centrifugation and then heated to or incubated at various temperatures, and the supernatant was removed for measurement of the EPR signal. A different aliquot of the sample was used for each treatment. The results are shown in Table VII (experiments 2 and 3). This method suffered the potential disadvantage that unbound Mn^{2+} within the pellet might not diffuse into the supernatant and be detectable. However, at least the entire supernatant could be thoroughly mixed after removal from the pellet, unlike the experiment where the temperature was varied directly in the spectrometer with the whole sample in the EPR capillary tube.

The difference in bound Mn^{2+} between states B and C was again found to be 2–3%, similar to the results found in experiment 1. The bound Mn^{2+} increased upon cooling rapidly to 4 °C but not to the level achieved by incubation at 65 °C (experiment 3, Table VII). Cooling to a low temperature (4 °C) followed by incubation at 65 °C caused more rebinding of Mn^{2+} (in 20 min) than cooling directly to 65 °C. Cooling to 37 °C followed by incubation at 65 °C was less effective. Results from two separate determinations were averaged for the data shown for experiment 3 in Table VII. Although the standard deviations indicate that differences in the bound Mn^{2+}:DPPG ratio following the different sample treatments are not significant, the same order of effectiveness in causing Mn^{2+} rebinding, (95 → 4 → 65 °C) > (95 → 37 → 65 °C) = (95 → 65 °C) > (95 → 4 °C), was found in both determinations.

This was confirmed by further experiments in which the pelleted sample was subjected to different temperature treatments directly in the EPR spectrometer. The pellet was positioned in the center of the spectrometer cavity so that changes in the Mn^{2+} concentration in the aqueous phase in the vicinity of the pellet were measured. This gave the type of spectrum shown in Figure 1C,D. Changes in the height of the spectrum due to free Mn^{2+} were measured at different temperatures and corrected for the temperature dependence by determining h_{sa}/h_{st} as described under Materials and Methods. The changes in h_{sa}/h_{st} under different conditions for a representative experiment (sample 1) are shown in Table VIII. The free Mn^{2+} concentration is highest at 92 °C in state C. On cooling to 20 °C where the sample is in state A, the free Mn^{2+} concentration decreases, indicating that some Mn^{2+} has become rebound on cooling. However, after incubation at 52 °C for 58 min to convert to state B, the free Mn^{2+} concentration decreases even further, indicating that the remaining Mn^{2+} which dissociated at 92 °C became rebound at 52 °C. On cooling back to 20 °C, h_{sa}/h_{st} is equal to that at 52 °C after 58 min and less than that on cooling directly to 20 °C from 92 °C. Thus, about half of the Mn^{2+} which dissociated at 92 °C became rebound on cooling to 20 °C, and the other half became rebound after incubation at 52 °C. On heating to 92 °C and cooling back to 20 °C, the free Mn^{2+} concentration again increases. This series of measurements is reproducible through several heating and cooling cycles, but eventually rebinding of the dissociated Mn^{2+} becomes less complete. Thus, the same sample could not be used for all the heating and cooling treatments described below. Spectra C and D of Figure 1 show typical differences in the free signal height between states A and B, respectively, at 20 °C. The relative height of the free to exchange-broadened signal depends on the ratio of the volumes of the pellet and aqueous phase and on the bulk ratio of Mn^{2+}:PG.

In order to determine at what temperatures Mn^{2+} became rebound on cooling, the rate of change in the free signal on cooling from 92 °C to different temperatures was determined.

Table VIII: Changes in Free Mn^{2+} Concentration at Different Temperatures and after Various Sample Treatments

sample	treatment	phase state	temp of measurement (°C)	h_{sa}/h_{st}
1	92 °C	C	92	0.10
	92 → 20 °C	A	20	0.08
	92 → 20 → 52 °C	A[a]	52	0.07
	52 °C for 58 min	B	52	0.05
	52 → 20 °C	B	20	0.05
	92 → 20 °C	A	20	0.07
2[b]	92 °C	C	92	0.16
	92 → 54 °C	A[a]	54	0.16
	54 °C for 37 min	A	54	0.15
	72 °C for 15 min	B	54	0.11
3[b]	92 °C	C	92	0.18
	92 → 24 °C	A[a]	24	0.17
	24 °C for 31 min	A	24	0.16
	72 °C for 15 min	B	24	0.11
4[b,c]	92 → 64 °C	A[a]	64	0.26
	64 °C for 47 min	B	64	0.16
	64 → 44 °C	B	44	0.16
	92 → 9 °C	A	9	0.31[d]
	92 → 9 → 64 °C	A[a]	64	0.19
	64 °C for 18 min	B	64	0.16
	64 → 9 °C	B	9	0.24[d]
	92 → 44 °C	A	44	0.23
	92 → 44 → 64 °C	A[a]	64	0.23
	64 °C for 63 min	B	64	0.16
	64 → 44 °C	B	44	0.16
	44 → 9 °C	B	9	0.23[d]

[a] Measurement made immediately after equilibration at the temperature indicated. [b] Samples used for Figure 6A. [c] Sample used for Figure 6B. [d] Ratios for sample 4 at higher temperatures can probably be compared to each other but not to the ratio at 9 °C. However, a decrease in the ratio at 9 °C after incubation at 64 °C compared to that on cooling directly from 92 °C indicates that rebinding of Mn^{2+} occurred during incubation.

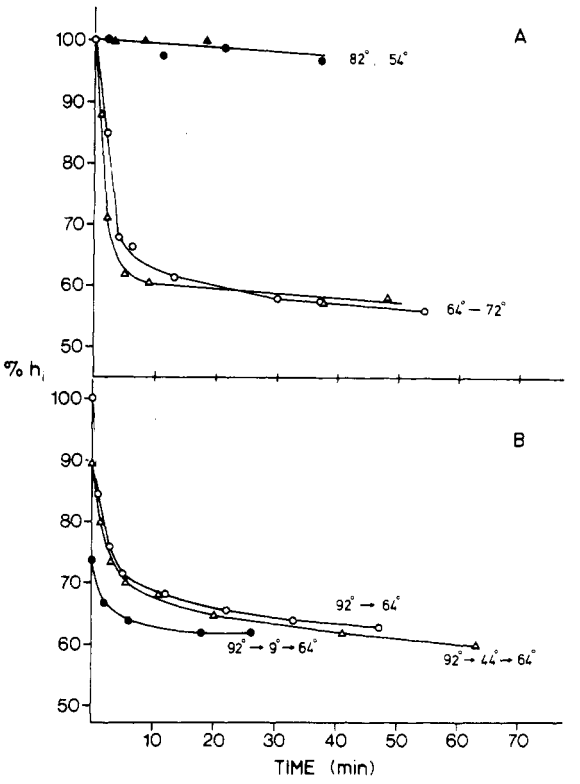

FIGURE 6: (A) Rate of change of free Mn^{2+} concentration in the presence of DPPG at different temperatures after cooling from 92 °C to the indicated temperature. The change in free Mn^{2+} concentration is measured from the height of the EPR spectrum and is expressed as the percentage of the height at zero time at the indicated temperature: 64 °C (○); 72 °C (△); 82 °C (▲); 54 °C (●). Temperatures below 54 °C gave the same result as 54 °C. (B) Rate of change of free Mn^{2+} concentration in the presence of DPPG at 64 °C after various sample treatments. The change in free Mn^{2+} concentration is expressed as the percentage of the height at zero time at 64 °C after cooling directly from 92 °C. (○) The sample is cooled from 92 °C directly to 64 °C. (△) The sample is cooled from 92 to 44 °C and then heated to 64 °C. (●) The sample is cooled from 92 to 9 °C and then heated to 64 °C. The signal height at 64 °C at zero time is measured immediately after equilibration at that temperature (0.001 M Mn^{2+}; bulk Mn^{2+}:PG ratio of 0.6:1).

The percent change in the free signal height relative to the height at zero time at each temperature is shown in Figure 6A. Rapid rebinding of Mn^{2+} occurred when the sample was cooled to 64 or 72 °C but not when cooled to 82 °C or when cooled rapidly to 54 °C or lower temperatures. The value of h_{sa}/h_{st} at 54 °C after cooling from 92 °C was similar to that at 92 °C as shown in Table VIII (sample 2), indicating not only that the free Mn^{2+} concentration did not change with time at 54 °C as shown in Figure 6A but also that it did not decrease during the cooling step from 92 to 54 °C before the first measurement at 54 °C could be made. Afer the temperature is raised back to 72 °C and the sample is incubated for 15 min to convert it to state B, h_{sa}/h_{st} at 54 °C is decreased due to rebinding of Mn^{2+} which occurred during the incubation at 72 °C. If the sample is cooled from 92 to 24 °C, however (Table VIII sample 3), h_{sa}/h_{st} is somewhat less than its value at 92 °C but not as low as after conversion to state B by incubation at 72 °C for 15 min. This indicates that some of the Mn^{2+} (16%) became rebound during the cooling step and some (11%) during incubation at 24 °C but that most of it did not become rebound until the sample was reheated and incubated at 72 °C.

The DSC results shown in Figure 2f,g indicated that the rate of conversion of state A to B is faster the lower the starting temperature. The effects of cooling to two different temperatures, 9 and 44 °C, on Mn^{2+} rebinding at 64 °C after reheating were compared as shown in Figure 6B. The height at 64 °C is expressed as a percentage of the initial height at 64 °C on cooling directly from 92 °C. Values of h_{sa}/h_{st} for the same sample (sample 4) at different temperatures are given in Table VIII. Other samples were taken repeatedly through the temperature cycles shown in Table VIII and Figure 6, and values of h_{sa}/h_{st} were reproducible to within 2–4% (data not shown).[2] The results in Figure 6B indicate that some of the Mn^{2+} became rebound during the cycle of cooling and reheating since the initial height at 64 °C was lower after this procedure than on cooling directly from 92 to 64 °C. More Mn^{2+} was found to be rebound at zero time at 64 °C after cooling to 9 °C than after cooling to 44 °C. The remaining Mn^{2+} then rebound slowly at a similar rate as the slow phase of Mn^{2+} rebinding on cooling directly from 92 to 64 °C.

Data presented in Table VIII for the same sample (sample 4) suggest that most of the Mn^{2+} which became rebound on taking the sample through the cooling and reheating cycle did so at or near 64 °C rather than at the low temperature. The values of h_{sa}/h_{st} at 9 and 44 °C were higher on cooling directly to either of these temperatures than after incubation at 64 °C and conversion to state B. Thus, for the sample cooled to 9 °C, the rapid phase of rebinding at 64 °C is already over by the time the first measurement is made but must have occurred while reheating to 64 °C. Studies of other samples showed that heating from 9 to 44 °C did not cause Mn^{2+} rebinding (data not shown),[2] so the Mn^{2+} must rebind between 44 and 64 °C. These results indicate that cooling to a lower temperature increases the rate of the rapid phase of Mn^{2+} rebinding at or near 64 °C.

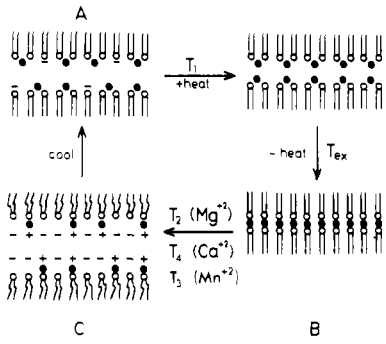

FIGURE 7: Diagrammatic representation indicating the structure of the hydrated metastable state A, dehydrated stable state B, and hydrated liquid-crystalline state C and the mechanism of conversion between them. Only half of each bilayer is shown. The transition from state B to state C is reversible at slow cooling rates for Ca^{2+} and Mn^{2+}. The unlettered state in the upper right-hand corner may not actually exist but indicates that the cation must rebind and neutralize the bilayer surfaces before state B can occur. The transition from state A to state B may occur during the exothermic transition, T_{ex}, at temperatures below T_1 at slow heating rates in the case of Ca^{2+} and Mn^{2+}. (●) Divalent cation.

Discussion

The earlier freeze–fracture electron microscopy, X-ray diffraction, and ^{31}P NMR results indicating that state B is in the form of dehydrated or nearly dehydrated sheets or cylinders in the presence of divalent cations suggest that the cations cause close contact of opposing bilayers in state B, probably by "trans"-type bridging of the lipids (Figure 7)—as proposed by Portis et al. (1979) for the dehydrated state of the Ca^{2+}–PS complex. The lower transition temperature of state B of the Mg^{2+} complex, relative to the Ca^{2+} complex, suggests that it may be less dehydrated than the Ca^{2+} complex. The different high-temperature phases of the Ca^{2+} complex may be due to varying degrees of dehydration. Close contact of the bilayers in state B would require complete neutralization of the lipid in order for the bilayers to approach each other and thus only occurs when there is sufficient divalent cation to bind in a 1:2 ratio. Cis-type bridging of adjacent lipids in the same bilayer by the cation probably occurs in the gel state at cation to lipid ratios less than 0.5:1 and in the metastable phase at higher cation ratios.

The fact that the transition temperatures of the metastable state on heating and of the liquid-crystalline phase on cooling are lower than those of the protonated form of the lipid, combined with the dependence of the rate of the transition to the stable state on the concentration of monovalent and divalent cations, suggested that some divalent cation dissociates from the lipid in state C, leaving the lipid incompletely neutralized, and does not rebind to state A at low temperatures, except perhaps very slowly. Since the lamellae in state A then have a small net negative charge, close contact of lamellae and formation of state B (Figure 7) cannot occur. The DSC results suggested that increased binding may occur gradually at temperatures above 50 °C if the sample is heated slowly, especially for Ca^{2+} and Mn^{2+}, or suddenly, after state A starts to melt, if the sample is heated quickly. They also suggested that Ca^{2+} and Mn^{2+} but not Mg^{2+} can rebind on cooling if the cooling rate is slow and that if rebinding occurs during cooling the sample freezes into one of the stable states and not the metastable state.

Measurement of changes in Mn^{2+} binding at different temperatures to the Mn^{2+}–DPPG complex at bulk ratios close to 0.5:1 from the EPR spectrum of free Mn^{2+} confirmed this hypothesis. The results showed that a small percentage of the Mn^{2+} (2–3% at 0.001M Mn^{2+}, bulk ratio of cation to lipid of 0.6:1) dissociates from the high-temperature liquid-crystalline phase. If the sample is cooled slowly, the Mn^{2+} is able to rebind at temperatures between 54 and 82 °C; the rate of rebinding is greatest between 64 and 72 °C. However, if the sample is cooled rapidly, most of the dissociated Mn^{2+} does not rebind during cooling nor at temperatures below 44 °C. The Mn^{2+} rebinds rapidly on reheating at or near 64 °C, close to the temperature of the endothermic transition of the metastable phase observed by DSC.

A reduction in affinity of the liquid-crystalline phase lipid for divalent cation was also shown by Puskin & Martin (1979) and is probably due to the inability of the cation to bridge the more expanded liquid-crystalline phase lipids by cis-type bridging as well as to the lower surface charge density. However, in their study, the divalent cation was present at a low mole ratio to lipid and rebound rapidly to the gel phase because the concentration of free lipid was high. At the higher cation to lipid ratios necessary to induce metastable phase behavior, the dissociated cation does not rebind rapidly to the metastable gel phase because the few molecules of unbound lipid present in state A are separated from each other by the much greater number of cation-bound lipids. There is a low propability of finding two unbound lipids adjacent to each other for binding to the cation in a 1:0.5 ratio by cis-type binding. Indeed, the less unbound lipid remaining, the lower its affinity for the cation will be.

However, as the sample is heated, increased translational motion of the lipids occurs, the probability of finding two unbound molecules of PG adjacent to each other increases, and more cation binds. If the sample is heated slowly, this can occur without melting of the metastable phase and at temperatures below 60 °C, at least for Ca^{2+} and Mn^{2+}, although perhaps not for Mg^{2+}. During the phase transition of the metastable phase, the lateral motion of the lipid is probably at a maximum, allowing rapid rebinding to the remaining dissociated divalent cation. Once the cation has become rebound and the surface is neutralized, close association of the bilayers, interlamellar trans bridging, and dehydration can recur, causing a release of heat. The amount of heat released during the exothermic process is enough to account for only about half of the excess enthalpy of state B relative to state A. Some additional change and release of heat must occur noncooperatively during cooling or at temperatures between T_1 and T_2. The decreased dependence of the T_m and ΔH of state B on fatty acid chain length suggests that the heat released upon dehydration is constant for each lipid and about 4–5 kcal/mol.

The inability of Mg^{2+} to rebind during slow cooling or at temperatures below the transition temperature of the metastable state on heating is due to the lower affinity of Mg^{2+}, relative to Ca^{2+} and Mn^{2+}. The absence of any dependence of the rate of the transition to state B on Ca^{2+} concentration, below 0.1 M even after rapid cooling, is probably due to the fact that it rebinds more rapidly during heating than Mg^{2+}. The Ca^{2+} is probably completely rebound by the time state A has been converted to state B′, and thus the rates of the transitions from B′ to B″ and B″ to B do not depend on Ca^{2+} rebinding. However, the degree of conversion to B″ and B does depend on the heating rate, indicating that these processes are slower than the rates of Ca^{2+} rebinding and of the first exothermic process. The increased conversion to state B seen at Ca^{2+} concentrations above 0.1 M may be due to increased rebinding during cooling even at the fast cooling rate used (20–40 °C/min).

The results also indicate that the lower the temperature to which the sample is cooled the faster is the rate of Mn^{2+} rebinding at or near the transition temperature of the metastable state A. This explains the greater rate of conversion to state B observed by DSC when the starting temperature is decreased. However, the reason for this faster rate of Mn^{2+} rebinding after cooling to a low temperature is not understood.

According to the model presented in Figure 7, the metastable phase behavior is due to dissociation of a small amount of the divalent cation from the liquid-crystalline phase and the inability of the cation to rebind to the lipid once it has gone into the gel state. Thus, this phenomenon is a consequence of fast cooling, at least for Ca^{2+} and Mn^{2+}. However, it may nonetheless be relevant to biological membranes. In biological membranes, there may be other factors which cause isolation and immobilization of individual molecules of acidic lipid which are not bound to divalent cations, as occurs in the metastable state of the cation–PG complex. An implication for biological processes of the model shown in Figure 7 is that divalent cations cannot cause lipid clustering unless cis-type bridging can occur, or fusion unless trans-type bridging can occur. In order to obtain close contact and fusion, the membrane surfaces, at least in the region which fuses, must be completely neutralized, and complete cation binding to all of the free acidic lipid must occur. This can only occur if the rate of translational motion is sufficiently high that two molecules of free acidic lipid are found adjacent to each other. The affinity of the lipid for the cation will decrease the more diluted the unbound lipid is by other membrane constituents and the lower the rate of its lateral motion. Thus, the affinity of some of the available acidic lipids in natural membranes for divalent cations may be much less than expected from measurements made on pure lipid vesicles at low cation to lipid ratios.

Registry No. Dimyristoylphosphatidylglycerol, 61361-72-6; dipalmitoylphosphatidylglycerol, 4537-77-3; distearoylphosphatidylglycerol, 4537-78-4; sodium, 7440-23-5; calcium, 7440-70-2; magnesium, 7439-95-4; manganese, 7439-96-5.

References

Bartlett, G. R. (1959) *J. Biol. Chem. 234*, 466.

Bligh, E. G., & Dyer, W. J. (1959) *Can. J. Biochem. 37*, 911.

Boggs, J. M., & Moscarello, M. A. (1978) *Biochemistry 17*, 5734.

Boggs, J. M., Wood, D. D., & Moscarello, M. A. (1981a) *Biochemistry 20*, 1065.

Boggs, J. M., Stamp, D., & Moscarello, M. A. (1981b) *Biochemistry 20*, 6066.

Boggs, J. M., Stamp, D., & Moscarello, M. A. (1982) *Biochemistry 21*, 1208.

Copeland, B. R., & Andersen, H. C. (1981) *J. Chem. Phys. 74*, 2548.

Copeland, B. R., & Andersen, H. C. (1982) *Biochemistry 21*, 2811.

Cullis, P. R., & de Kruijff, F. (1976) *Biochim. Biophys. Acta 436*, 523.

Farren, S. G., & Cullis, P. R. (1980) *Biochem. Biophys. Res. Commun. 97*, 182.

Findlay, E. J., & Barton, P. G. (1978) *Biochemistry 17*, 2400.

Fleming, B. D., & Keough, K. M. W. (1981) *Proc. Can. Fed. Biol. Soc. 24*, 103a.

Fleming, B. D., & Keough, K. M. W. (1983) *Can. J. Biochem.* (in press).

Galla, H. J., & Sackmann, E. (1975) *Biochim. Biophys. Acta 401*, 509.

Harlos, K., & Eibl, H. (1980a) *Biochemistry 19*, 895.

Harlos, K., & Eibl, H. (1980b) *Biochim. Biophys. Acta 601*, 113.

Hauser, H., & Shipley, G. G. (1983) *Biophys. J. 41*, 119a.

Jacobson, K., & Papahadjopoulos, D. (1975) *Biochemistry 14*, 152.

Liao, M. J., & Prestegard, J. H. (1981) *Biochim. Biophys. Acta 645*, 149.

Papahadjopoulos, D. (1977) *J. Colloid Interface Sci. 58*, 459.

Papahajopoulos, D., Jacobson, K., Nir, S., & Isac, T. (1973) *Biochim. Biophys. Acta 311*, 330.

Papahadjopoulos, D., Vail, W. J., Jacobson, K., & Poste, G. (1975) *Biochim. Biophys. Acta 394*, 483.

Paphadjopoulos, D., Vail, W. J., Newton, C., Nir, S., Jacobson, K., Poste, G., & Lazo, R. (1977) *Biochim. Biophys. Acta 465*, 579.

Portis, A., Newton, C., Pangborn, W., & Papahadjopoulos, D. (1979) *Biochemistry 18*, 780.

Puskin, J. S. (1977) *J. Membr. Biol. 35*, 39.

Puskin, J. S., & Martin, T. (1979) *Biochim. Biophys. Acta 552*, 53.

Sacrê, M.-M., Hoffmann, W., Turner, M., Tocanne, J.-F., & Chapman, D. (1979) *Chem. Phys. Lipids 69*, 69.

van Dijck, P. W. M., Ververgaert, P. H. J. Th., Verkleij, A. J., van Deenen, L. L. M., & de Geer, J. (1975) *Biochim. Biophys. Acta 406*, 465.

van Dijck, P. W. M., de Kruijff, B., Verkleij, A. J., van Deenen, L. L. M., & de Geer, J. (1978) *Biochim. Biophys. Acta 512*, 84.

Verkleij, A. J., de Kruijff, B., Ververgaert, P. H. J. Th., Tocanne, J. F., & van Deenen, L. L. M. (1974) *Biochim. Biophys. Acta 339*, 432.

Ververgaert, P. H. J. Th., de Kruijff, B., Verkleij, A. J., Tocanne, J. F., & van Deenen, L. L. M. (1975) *Chem. Phys. Lipids 14*, 97.